ORIGINAL PAPER

Analyses of the driver's anticipation effect in a new lattice hydrodynamic traffic flow model with passing

Arvind Kumar Gupta · Poonam Redhu

Abstract In this paper, we studied the effect of driver's anticipation with passing in a new lattice model. The effect of driver's anticipation is examined through linear stability analysis and shown that the anticipation term can significantly enlarge the stability region on the phase diagram. Using nonlinear stability analysis, we obtained the range of passing constant for which kink soliton solution of mKdV equation exist. For smaller values of passing constant, uniform flow and kink jam phase are present on the phase diagram and jamming transition occurs between them. When passing constant is greater than the critical value depending on the anticipation coefficient, jamming transitions occur from uniform traffic flow to kink-bando traffic wave through chaotic phase with decreasing sensitivity. The theoretical findings are verified using numerical simulation which confirm that traffic jam can be suppressed efficiently by considering the anticipation effect in the new lattice model.

Keywords Traffic flow · Driver's anticipation effect · Chaotic jam

A. K. Gupta (✉) · P. Redhu
Indian Institute of Technology Ropar,
Rupnagar 140001, Punjab, India
e-mail: akgupta@iitrpr.ac.in

P. Redhu
e-mail: poonamr@iitrpr.ac.in

1 Introduction

In recent years, due to rapid increase of automobiles on the roads, the problem of traffic jam has attracted considerable attention of scientists and researchers. To investigate the properties of traffic congestion and also to reduce it, a lot of mathematical models [1–12] have been proposed. Nagatani [13] firstly introduced a lattice hydrodynamic model in which drivers adjust their velocity according to the observed headway. Later, many extended version of Nagatani's lattice models have been developed by considering different factors like backward effect [14], lateral effect of the lane width [15] and anticipation effect of potential lane changing [16] etc. Recently, Peng [17] proposed a new lattice model by incorporating the effect of anticipation individual driving behavior. Kang and Sun [18] introduced a lattice hydrodynamic model by taking into account driver's delay effect in sensing relative flux (DDSRF) and found that this effect has an important influence on the traffic jams. Most of the above cited models describe some traffic phenomena only on single lane.

Furthermore, Nagatani [19] also extended his original lattice model to two-lane traffic system and analyzed the lane changing behavior. Afterwards, in this direction some modifications have also been proposed by considering optimal current difference [20], flow difference effect [21], density difference effect [22] and effect of driver's anticipation [23] in two-lane system. Recently, Gupta and Redhu [24] devel-

oped a new model by considering driver's anticipation effect in sensing relative flux (DAESRF) in a two-lane system.

In real traffic, drivers often adjust their velocity according to the observed traffic situations and always estimate their driving behavior. Therefore, driver's anticipation effect plays an important role in stabilizing and destabilizing the traffic flow. In a traffic network, faster moving vehicles always try to overtake slower moving vehicles to maintain their optimal speed. In this direction, Nagatani [25] extended his lattice hydrodynamic model to take into account the passing effect. systems, driver's anticipation effect plays an important role. But, upto our knowledge the effect of driver's anticipation has not been studied in traffic systems with passing.

The paper is organized as follows: in the following section, a more realistic lattice model considering driver's anticipation behavior with passing effect for a single lane is proposed. In Sect. 3, the linear stability analysis is performed for the proposed model. Section 4 is devoted to the nonlinear analysis in which mKdV equation is derived. Numerical simulations are carried out in Sect. 5 and finally, conclusions are given in Sect. 6.

2 Proposed model

Nagatani [13] introduced the first lattice hydrodynamic model by incorporating the idea of microscopic optimal velocity model to analyze the density wave of traffic flow and is given by

$$\partial_t \rho_j + \rho_0 \left(\rho_j v_j - \rho_{j-1} v_{j-1} \right) = 0, \tag{1}$$

$$\partial_t (\rho_j v_j) = a \left[\rho_0 V(\rho_{j+1}) - \rho_j v_j \right], \tag{2}$$

where j indicates site-j on the one-dimensional lattice; ρ_j and v_j, respectively, represent the local density and velocity at site-j at time t; ρ_0 is the average density; $a(= 1/\tau)$ is the sensitivity of drivers; $V(\cdot)$ is called optimal velocity function and it is taken as

$$V(\rho) = \frac{V_{\max}}{2} \left[\tanh\left(\frac{2}{\rho_0} - \frac{\rho}{\rho_0^2} - \frac{1}{\rho_c} \right) + \tanh\left(\frac{1}{\rho_c} \right) \right], \tag{3}$$

here $V_{\max}$ and ρ_c denote the maximal velocity and the safety critical density, respectively. This optimal velocity function is monotonically decreasing, has an upper bound and an inflection point at $\rho = \rho_c = \rho_0$.

The above model is further extended to take passing effect into account by Nagatani [25]. The continuity equation remain preserved even in passing case while the evolution equation is modified by looking at the difference of traffic currents on site-j and $j + 1$. When the traffic current on site-j is larger than the current on site-$j + 1$, passing occurs and is proportional to the difference between the optimal currents at site-j and $j + 1$. Then, the modified evolution equation by considering passing effect is given by

$$\partial_t (\rho_j v_j) = a \left[\rho_0 V(\rho_{j+1}) - \rho_j v_j \right] \\ + a\gamma \left[\rho_0 V(\rho_{j+1}(t)) - \rho_0 V(\rho_{j+2}(t)) \right], \tag{4}$$

where, γ is a passing constant.

As observed in real traffic flow, drivers always adjust their vehicles based on the available dynamic estimation information and then take decisions after some time. Suppose drivers sense the traffic relative information at time t and make a decision to adjust their velocity at a later time $t + \tau_1$, where τ_1 is the delay of driver's response in sensing headway. Then, due to the delay of car motion, vehicles move at a later time $t + \tau_1 + \tau_2$, where τ_2 is the delay time of vehicles motion. So, the total delay time can be divided into two parts τ_1 and τ_2. For simplicity, we choose the linear relationship between driver's response delay τ_1 and the total delay time τ as $\tau_1 = \alpha \tau$, where α is the anticipation coefficient corresponds to driver behavior and $\tau = 1/a$ denote the delay time which allows for the time lag, that it takes the traffic current to reach the optimal current when the traffic is varying. However, the above discussed driver's anticipation effect was not considered in the lattice model with passing. In view this, we proposed a new evolution equation with consideration of driver's anticipation effect on one-dimensional traffic flow when passing is allowed as follows:

$$\partial_t (\rho_j v_j) = a \left[\rho_0 V(\rho_{j+1}(t + \alpha\tau)) - \rho_j v_j \right] \\ + a\gamma \left[\rho_0 V(\rho_{j+1}(t + \alpha\tau)) \\ - \rho_0 V(\rho_{j+2}(t + \alpha\tau)) \right]. \tag{5}$$

Based on the sign of anticipation coefficient α, the above equation can explore different characteristics of driver's anticipation behavior on a single lane highway. Here, $\alpha > 0$ represents anticipation driving behavior or the driver's forecast effect in a traffic system with ITS. The idea is that drivers adjust their driving speeds to the anticipation optimal speed at time $t + \alpha\tau$ after

delay time τ in advance. So, the bigger value of α corresponds to skillful drivers in the model.

For $\alpha < 0$, i.e. negative anticipation coefficient corresponds to the explicit driver's physical delay in sensing relative flux. When $\alpha = 0$, the new model reduces to Nagatani's [25] model. For simplicity, using the Taylor series expansion and neglecting the non-linear terms, the new evolution equation can be obtained as follows:

$$
\begin{aligned}
&\partial_t(\rho_j(t)v_j(t)) \\
&= a\rho_0\left[V\left(\rho_{j+1}(t)\right) + \alpha\tau V'(\rho_{j+1})\partial_t\rho_{j+1}(t)\right. \\
&\quad \left. - \rho_j(t)v_j(t)\right] \\
&\quad + a\rho_0\gamma\left[\Delta V\left(\rho_{j+1}(t)\right) + \alpha\tau\left(V'(\rho_{j+1}(t))\right.\right. \\
&\quad \left.\left. \times \partial_t\rho_{j+1}(t) - V'\left(\rho_{j+2}(t)\right)\partial_t\rho_{j+2}(t)\right)\right]
\end{aligned}
\tag{6}
$$

where $\Delta V(\rho_j(t)) = V(\rho_{j+1}(t)) - V(\rho_{j+2}(t))$. By taking the difference form of Eqs. (1) and (6) and eliminating speed v_j, the evolution equation of density is obtained as

$$
\begin{aligned}
&\rho_j(t+2\tau) \\
&= \rho_j(t+\tau) - \tau\rho_0^2\left[V\left(\rho_{j+1}(t)\right) - V(\rho_j(t))\right] \\
&\quad - \tau\rho_0^2\alpha\left[V'\left(\rho_{j+1}(t)\right)\tilde{\Delta}\rho_{j+1}(t)\right. \\
&\quad \left. - V'(\rho_j(t))\tilde{\Delta}\rho_j(t)\right] \\
&\quad - \tau\rho_0^2\gamma\left[2V\left(\rho_{j+1}(t)\right) - V(\rho_{j+2}(t)) - V(\rho_j(t))\right] \\
&\quad - \tau\alpha\gamma\rho_0^2\left[2V'\left(\rho_{j+1}(t)\right)\tilde{\Delta}\rho_{j+1}(t)\right. \\
&\quad \left. - V'(\rho_{j+2}(t))\tilde{\Delta}\rho_{j+2}(t) - V'(\rho_j(t))\tilde{\Delta}\rho_j(t)\right],
\end{aligned}
\tag{7}
$$

where $\tilde{\Delta}\rho_j(t) = \rho_j(t+\tau) - \rho_j(t)$, $V'(\rho_j) = dV/d\rho_j$.

3 Linear stability analysis

To investigate the effect of driver's anticipation on traffic flow when passing is allowed, we conducted linear stability analysis in this section. The traffic density and optimal velocity under uniform traffic condition is taken as ρ_0 and $V(\rho_0)$, respectively, where ρ_0 is a constant. Hence, the steady-state solution of the homogeneous traffic flow is given by

$$
\rho_j(t) = \rho_0, \quad V_j(t) = V(\rho_0).
\tag{8}
$$

Let $y_j(t)$ be a small perturbation to the steady-state density on site-j. Then,

$$
\rho_j(t) = \rho_0 + y_j(t).
\tag{9}
$$

Substituting $\rho_j(t) = \rho_0 + y_j(t)$ in Eq. (7), we obtain

$$
\begin{aligned}
&y_j(t+2\tau) - y_j(t+\tau) + \tau\rho_0^2 V'(\rho_0)\Delta y_j(t) \\
&\quad + \tau\rho_0^2\alpha V'(\rho_0)\tilde{\Delta}(\Delta y_j(t)) - 2\tau\rho_0^2\gamma V'(\rho_0)\Delta^2 y_j(t) \\
&\quad - 2\tau\alpha\gamma\rho_0^2 V'(\rho_0)\Delta^2(\tilde{\Delta} y_j(t)) = 0,
\end{aligned}
\tag{10}
$$

where $\Delta y_j(t) = y_{j+1}(t) - y_j(t)$, $\tilde{\Delta} y_j(t) = y_j(t+\tau) - y_j(t)$.

Putting $y_j(t) = exp(ikj + zt)$ in Eq. (10), we get

$$
\begin{aligned}
&\mathrm{e}^{2\tau z} - \mathrm{e}^{\tau z} + \tau\rho_0^2 V'(\rho_0)\left(\mathrm{e}^{ik} - 1\right) \\
&\quad + \tau\rho_0^2\alpha V'(\rho_0)\left(\mathrm{e}^{ik} - 1\right)\left(\mathrm{e}^{\tau z} - 1\right) \\
&\quad + \tau\alpha\gamma\rho_0^2 V'(\rho_0)\left(2\mathrm{e}^{2ik}\left(\mathrm{e}^{\tau z} - 1\right)\right. \\
&\quad - \mathrm{e}^{2ik}\left(\mathrm{e}^{2ik+\tau z} - \mathrm{e}^{2ik}\right) - \left(\mathrm{e}^{\tau z} - 1\right) \\
&\quad \left. - \tau\rho_0^2\gamma V'(\rho_0)\left(1 - \mathrm{e}^{ik}\right)^2\right) = 0.
\end{aligned}
\tag{11}
$$

Inserting $z = z_1(ik) + z_2(ik)^2 \cdots$ into Eq. (11), we obtained the first and second-order terms of the coefficient ik and $(ik)^2$, respectively, as

$$
z_1 = -\rho_0^2 V'(\rho_0),
\tag{12}
$$

$$
\begin{aligned}
z_2 &= -\frac{3\tau z_1^2}{2} - \frac{\rho_0^2 V'(\rho_0)}{2} - \tau\alpha\rho_0^2 V'(\rho_0)z_1 \\
&\quad + \gamma\rho_0^2 V'(\rho_0).
\end{aligned}
\tag{13}
$$

When $z_2 < 0$, the uniform steady-state flow becomes unstable for long-wavelength waves. For $z_2 > 0$ the uniform flow will remain stable. Thus, the neutral stability curve is given by

$$
\tau = -\frac{1 - 2\gamma}{\rho_0^2 V'(\rho_0)(3 - 2\alpha)}.
\tag{14}
$$

The instability condition for the homogeneous traffic flow can be described as

$$
\tau > -\frac{1 - 2\gamma}{\rho_0^2 V'(\rho_0)(3 - 2\alpha)}.
\tag{15}
$$

Equation (15) clearly shows that anticipation coefficient α plays an important role in stabilizing the traffic flow when passing is considered. Solid curves in Fig. 1a, b is the neutral stability curves in the phase space corresponding to $\gamma = 0.06$ and $\gamma = 0.3$, respectively, for different values of α. The apex of each curve indicates the critical point. It can be easily depicted from the figure that the amplitude of these curves decreases with an increase in α which means that

Fig. 1 Phase diagram in parameter space (ρ, a) for **a** $\gamma = 0.06$, and **b** $\gamma = 0.3$
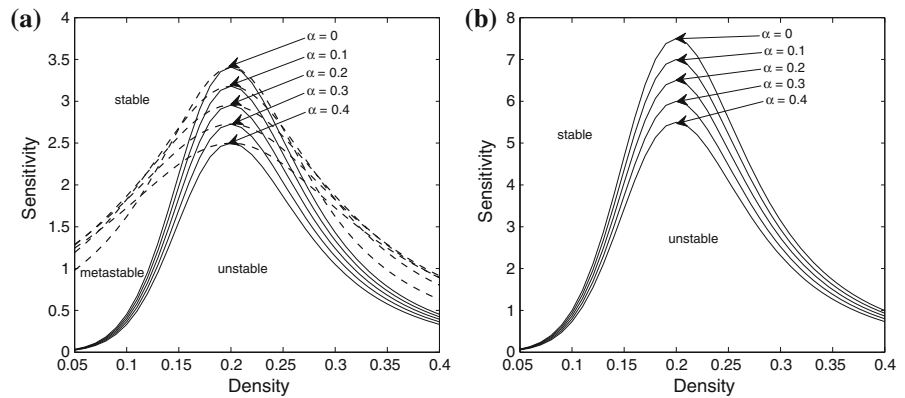
larger value of α leads to enlargement of stability region and hence, the traffic jam is suppressed efficiently. On comparing Fig. 1a, b, it is found that the stable region reduces for larger value of the passing coefficient.

4 Nonlinear stability analysis

Using reduction perturbation method, now, we investigate the evolution characteristics of traffic jam around the critical point (ρ_c, a_c) on coarse-grained scales. Long-wavelength expansion method is used to understand the slowly varying behavior near the critical point. The slow variables X and T for a small positive scaling parameter ϵ $(0 < \epsilon \ll 1)$ are defined as

$$X = \epsilon(j + bt), \quad T = \epsilon^3 t, \tag{16}$$

where b is a constant to be determined. Let ρ_j satisfy the following equation:

$$\rho_j(t) = \rho_c + \epsilon R(X, T). \tag{17}$$

By expanding Eq. (7) to fifth order of ϵ with the help of Eqs. (16) and (17), we obtain the following nonlinear equation:

$$
\begin{aligned}
&\epsilon^2 \left(b + \rho_c^2 V'\right) \partial_X R \\
&+ \epsilon^3 \left(\frac{3}{2} b^2 \tau + \frac{\rho_c^2 V'}{2} - \alpha \tau b \rho_c^2 V' - \gamma \rho_c^2 V'\right) \partial_X^2 R \\
&+ \epsilon^4 \begin{pmatrix} \partial_T R + \left(\frac{7}{6} b^3 \tau^2 + \frac{\alpha \rho_c^2 V'}{2}\left(b\tau + b^2\tau^2\right) \\ -\gamma \rho_c^2 V' - \tau \alpha b \rho_c^2 V' + \frac{\rho_c^2 V'}{6}\right) \partial_X^3 R + \frac{\rho_c^2 V'''}{6} \partial_X R^3 \end{pmatrix} \\
&+ \epsilon^5 \begin{pmatrix} \left(3b\tau + \alpha\tau\rho_c^2 V'\right)\partial_T \partial_X R + \frac{\gamma(1-2\gamma)\rho_c^2 V'''}{6}\partial_X^2 R^3 \\ + \left(\frac{5}{8}b^4\tau^3 + \frac{\alpha\tau\rho_c^2 V'}{6}\left(b\tau + 6\frac{b^2\tau^2}{4} + \frac{b^3\tau^3}{1}\right) - \frac{7}{12}\gamma\rho_c^2 V' \\ -\alpha\gamma\rho_c^2 V'\left(-\frac{1}{2}b^2\tau^2 - b\tau\right) + \frac{\rho_c^2 V'}{24}\right)\partial_X^4 R, \end{pmatrix} \\
&= 0, \tag{18}
\end{aligned}
$$

where $V' = \frac{\mathrm{d}V(\rho)}{\mathrm{d}\rho}|_{\rho=\rho_c}$, $V''' = \frac{\mathrm{d}V^3(\rho)}{\mathrm{d}\rho^3}|_{\rho=\rho_c}$. Near the critical point (ρ_c, a_c), the value of τ is set as

$$\tau = \tau_c(\epsilon^2 + 1). \tag{19}$$

By taking $b = -\rho_c^2 V'(\rho_c)$ and eliminating the second and third-order terms of ϵ, we obtain

$$
\begin{aligned}
&\epsilon^4 \left(\partial_T R - \left(-\frac{12\alpha^2\gamma^2 - 24\gamma^2\alpha + 14\gamma^2 - 12\alpha\gamma + 13\gamma + \alpha^2 - 1}{3(2\alpha - 3)^2}\right)\right. \\
&\left. \times \left(-\rho_c^2 V'\right)\partial_X^3 R + \frac{\rho_c^2 V'''}{6}\partial_X R^3\right) \\
&+ \epsilon^5 \begin{pmatrix} -\left(\frac{3-6\gamma-6\alpha-4\alpha^2}{4(3-2\alpha)}\right)\rho_c^2 V'\partial_X^2 R + \left(\frac{3-6\gamma}{12(2\alpha-3)}\right)\rho_c^2 V'''\partial_X^2 R^3 \\ +(16\gamma^4\alpha + 4\gamma^3(12\alpha^2 - 24\alpha - 11) \\ -6\gamma^2(16\alpha^3 - 40\alpha^2 + 26\alpha - 17) \\ +2\gamma(52\alpha^3 - 184\alpha^2 + 221\alpha - 111) \\ -4\alpha^3 + 10\alpha^2 - 9\alpha + 10)\left(\frac{-\rho_c^2 V'}{12(2\alpha-3)^3}\right)\partial_X^4 R \end{pmatrix} = 0 \\
&\tag{20}
\end{aligned}
$$

In order to drive the standard mKdV equation, we make the following transformation in Eq. (20):

$$
\begin{aligned}
T' &= \left(-\frac{12\alpha^2\gamma^2 - 24\gamma^2\alpha + 14\gamma^2 - 12\alpha\gamma + 13\gamma + \alpha^2 - 1}{3(2\alpha - 3)^2}\right. \\
&\left. \times \left(-\rho_c^2 V'\right)\right) T, \\
R &= \left(\frac{-2(12\alpha^2\gamma^2 - 24\gamma^2\alpha + 14\gamma^2 - 12\alpha\gamma + 13\gamma + \alpha^2 - 1)}{V'''(2\alpha - 3)^2}V'\right)^{\frac{1}{2}} R', \\
&\tag{21}
\end{aligned}
$$

with the existence condition as

$$-12\alpha^2\gamma^2 + 24\gamma^2\alpha - 14\gamma^2 + 12\alpha\gamma - 13\gamma - \alpha^2 + 1 > 0. \tag{22}$$

After applying above transformation, Eq. (20) becomes

$$\partial_{T'} R' = \partial_X^3 R' - \partial_X R'^3$$
$$- \epsilon \left[\frac{g_3}{g_1} \partial_X^2 R' + \frac{g_4}{g_1} \partial_X^4 R' + \frac{g_5}{g_2} \partial_X^2 R'^3 \right], \quad (23)$$

where

$$g_1 = -\frac{12\alpha^2\gamma^2 - 24\gamma^2\alpha + 14\gamma^2 - 12\alpha\gamma + 13\gamma + \alpha^2 - 1}{3(2\alpha - 3)^2}$$
$$\times \left(-\rho_c^2 V' \right)$$

$$g_2 = \frac{\rho_c^2 V'''}{6}, \quad g_3 = -\frac{3 - 6\gamma - 6\alpha - 4\alpha^2}{4(3 - 2\alpha)} \rho_c^2 V'$$

$$g_4 = \Big[16\gamma^4\alpha + 4\gamma^3(12\alpha^2 - 24\alpha - 11)$$
$$- 6\gamma^2(16\alpha^3 - 40\alpha^2 + 26\alpha - 17)$$
$$+ 2\gamma(52\alpha^3 - 184\alpha^2 + 221\alpha - 111)$$
$$- 4\alpha^3 + 10\alpha^2 - 9\alpha + 10 \Big] \frac{\left(-\rho_c^2 V' \right)}{12(2\alpha - 3)^3}$$

$$g_5 = \left(\frac{3 - 6\gamma}{2\alpha - 3} \right) \frac{\rho_c^2 V'''}{12}$$

After ignoring the $o(\epsilon)$ terms in Eq. (23), we get mKdV equation whose desired kink soliton solution is given by

$$R'_0(X, T') = \sqrt{c} \tanh \sqrt{\frac{c}{2}} (X - cT'). \quad (24)$$

In order to determine the value of propagation velocity for the kink–antikink solution, it is necessary to satisfy the solvability condition:

$$\left(R'_0, M[R'_0] \right) \equiv \int_{-\infty}^{\infty} dX R'_0 M \left[R'_0 \right] = 0, \quad (25)$$

with $M[R'_0] = M[R']$. By solving Eq. (23), the selected value of c is

$$c = \frac{5g_2 g_3}{2g_2 g_4 - 3g_1 g_5}. \quad (26)$$

Hence, the kink–antikink solution is given by

$$\rho_j = \rho_c + \epsilon \sqrt{\frac{g_1 c}{g_2}} \tanh \left(\sqrt{\frac{c}{2}} (X - cg_1 T) \right), \quad (27)$$

with $\epsilon^2 = \frac{a_c}{a} - 1$ and the amplitude A of the solution is

$$A = \sqrt{\frac{g_1}{g_2} \epsilon^2 c}. \quad (28)$$

The above kink solution exist only if condition (22) is satisfied. So the existence condition for kink solution is

$$0 \leq \gamma < \eta(\alpha), \quad (29)$$

where

$$\eta(\alpha) = \frac{12\alpha - 13 + \sqrt{(-(2\alpha^2 - 3)^2(12\alpha^2 + 12\alpha - 25))}}{4(6\alpha^2 - 9\alpha + 7)}. \quad (30)$$

For $\gamma \geq \eta(\alpha)$, the mKdV equation (23) cannot be derived from above nonlinear analysis. The kink–antikink solution represents the coexisting phase including both congested phase and freely moving phase which can be described by $\rho_j = \rho_c \pm A$, respectively, in the phase space (ρ, a) for $\gamma < \eta(\alpha)$. The dashed lines in Fig. 1a represent the coexisting curves which divide the phase plane into three regions: stable, metastable and unstable. In the stable region, the traffic flow will remain stable under a disturbance while in metastable and unstable region; a small disturbance will lead to the congested traffic. From Fig. 1a, it is clear that with an increase of anticipation coefficient α, the corresponding neutral and coexisting curves both lower down, which means that α can stabilize the traffic flow. For $\gamma = 0.3$, as the condition $\gamma \geq \eta(\alpha)$, is not satisfied, coexisting curers do not exist and are not shown in Fig. 1b for $\gamma = 0.3$. Figure 2a shows the phase diagram in parameter space (γ, a) for different values of α. Curves $a_c = (3 - 2\alpha)/(1 - 2\gamma)$, predicated by the linear stability analysis, represent the phase boundaries between no jam and kink jam for $\gamma < \eta(\alpha)$ and no jam with chaotic jam for $\gamma \geq \eta(\alpha)$. The modified Korteweg de Varies equation (23) has a kink–antikink soliton solution only for $\gamma < \eta(\alpha)$, therefore there exist only two regions no jam and kink jam for $\gamma < \eta(\alpha)$ in the phase plane. It is also clear from Fig. 2a that kink region reduces with an increase in the value of α for $\gamma < \eta(\alpha)$. This findings is in accordance with the results obtained in Ref. [24] that traffic jam suppressed efficiently by considering driver's anticipation effect. For $\gamma \geq \eta(\alpha)$, based upon the kinds of density wave, the unstable region is further divided into two subregions: kink jam and chaotic jam. The boundary between
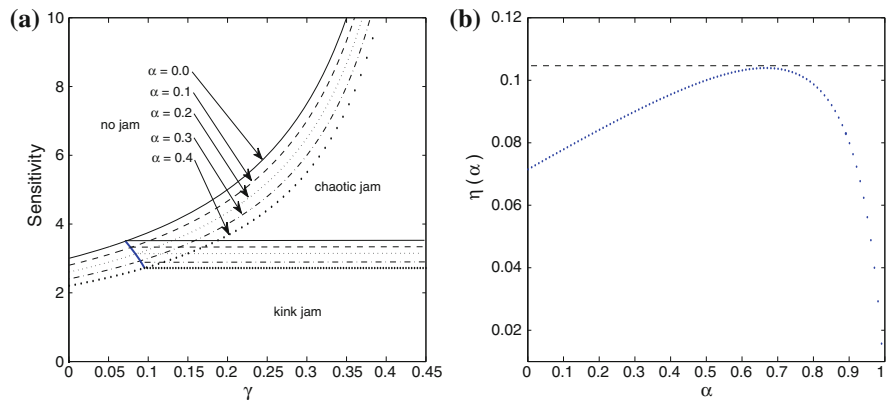
Fig. 3 Spatiotemporal
evolutions of density when
$\gamma = 0.06$ for $a = 2.7$
a $\alpha = 0$, **b** $\alpha = 0.1$,
c $\alpha = 0.2$, **d** $\alpha = 0.3$, and
e $\alpha = 0.4$, respectively
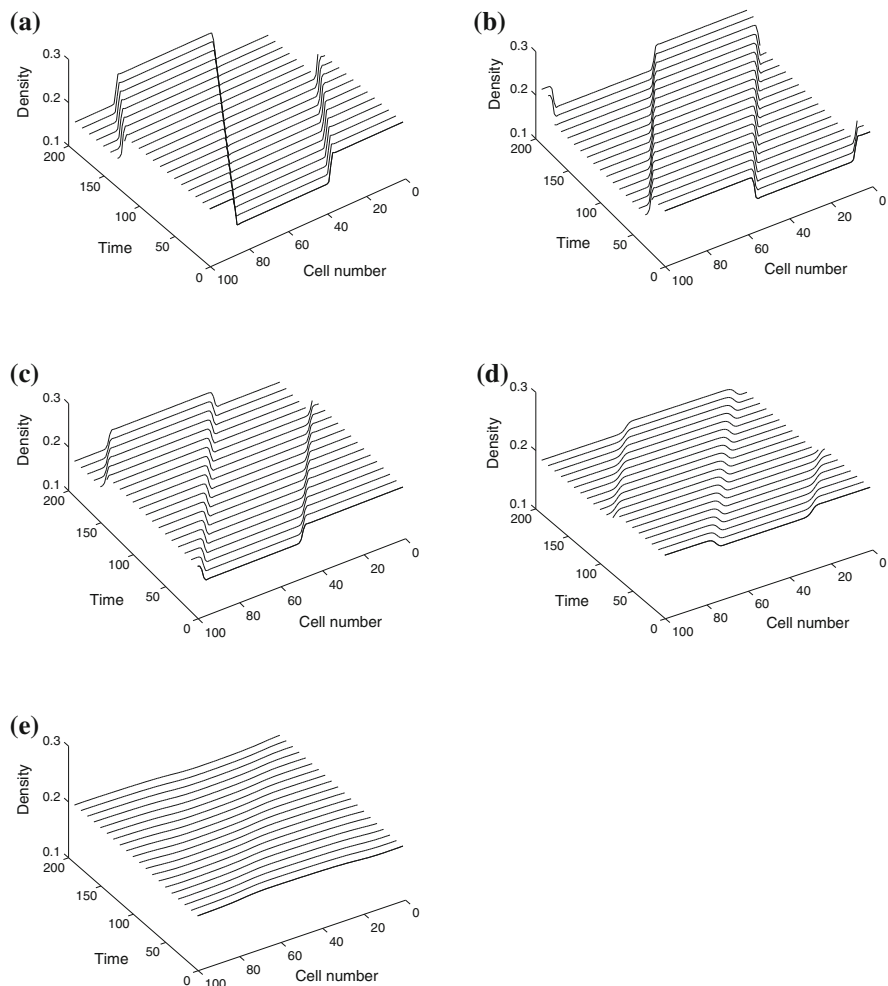
kink and chaotic jam is the line $a = (3-2\alpha)/(1-2\eta)$.
It is worth to mention here that for $\alpha = 0$, the results are
similar to those obtained in Ref. [25]. The driver's antic-

ipation effect also plays an important role when passing
rate is high ($\gamma \geq \eta(\alpha)$). The increase in the value of
α enlarges the free flow region while the chaotic and

Fig. 4 Density profiles at time $t = 20,200$ when $\gamma = 0.06$ for $a = 2.7$ **a** $\alpha = 0$, **b** $\alpha = 0.1$, **c** $\alpha = 0.2$, **d** $\alpha = 0.3$, and **e** $\alpha = 0.4$, respectively
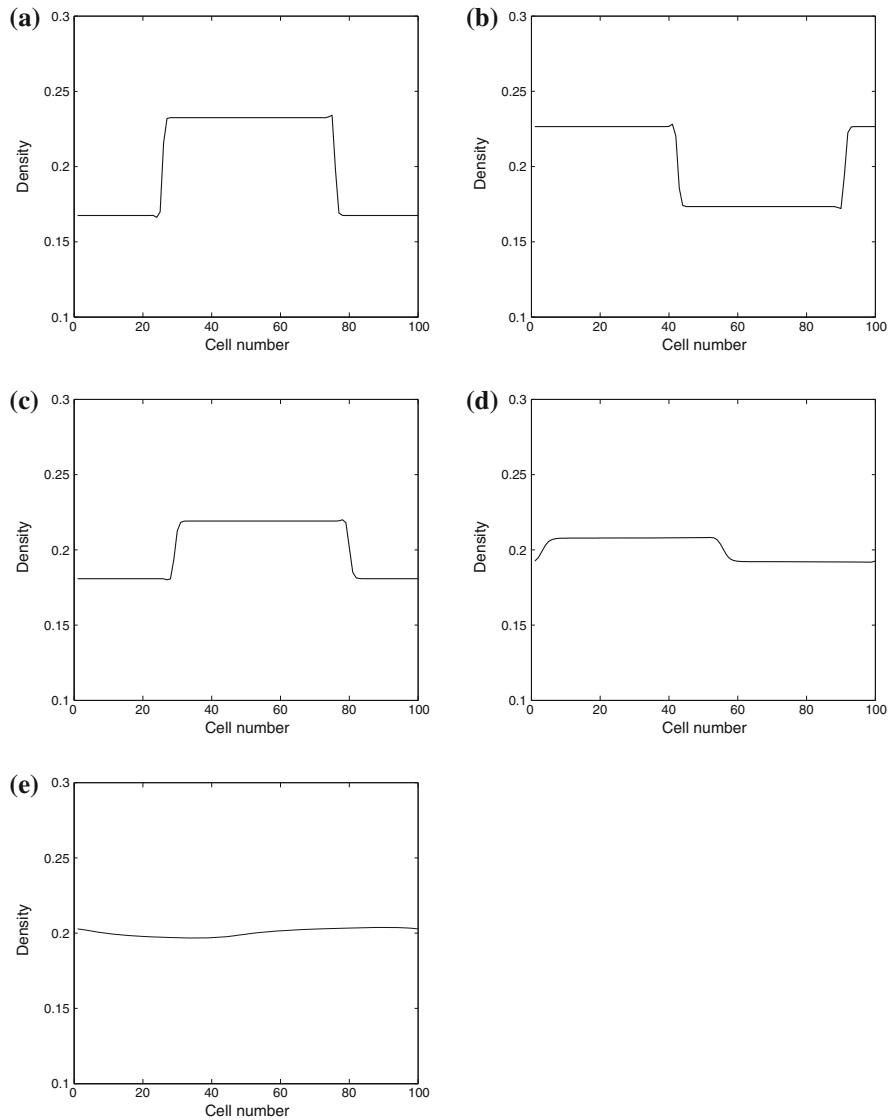
kink jam region reduces. Figure 2b, depicts the relationship between driver's anticipation effect with the critical value of γ. It is clear from the figure that the value of $\eta(\alpha)$ firstly increases with respect to α and then decreases sharply to zero as soon as $\alpha = 1$.

5 Numerical simulation

To check whether the proposed model is capable of describing the role of driver's anticipation effect on traffic flow dynamics with passing and validate linear as well as nonlinear stability analysis, numerical simulation is carried out for the proposed model under peri-

odic boundary conditions. To study the chaotic behavior in the proposed lattice model, we use nonrandom initial conditions. Initially, we defined density in term of a step function as
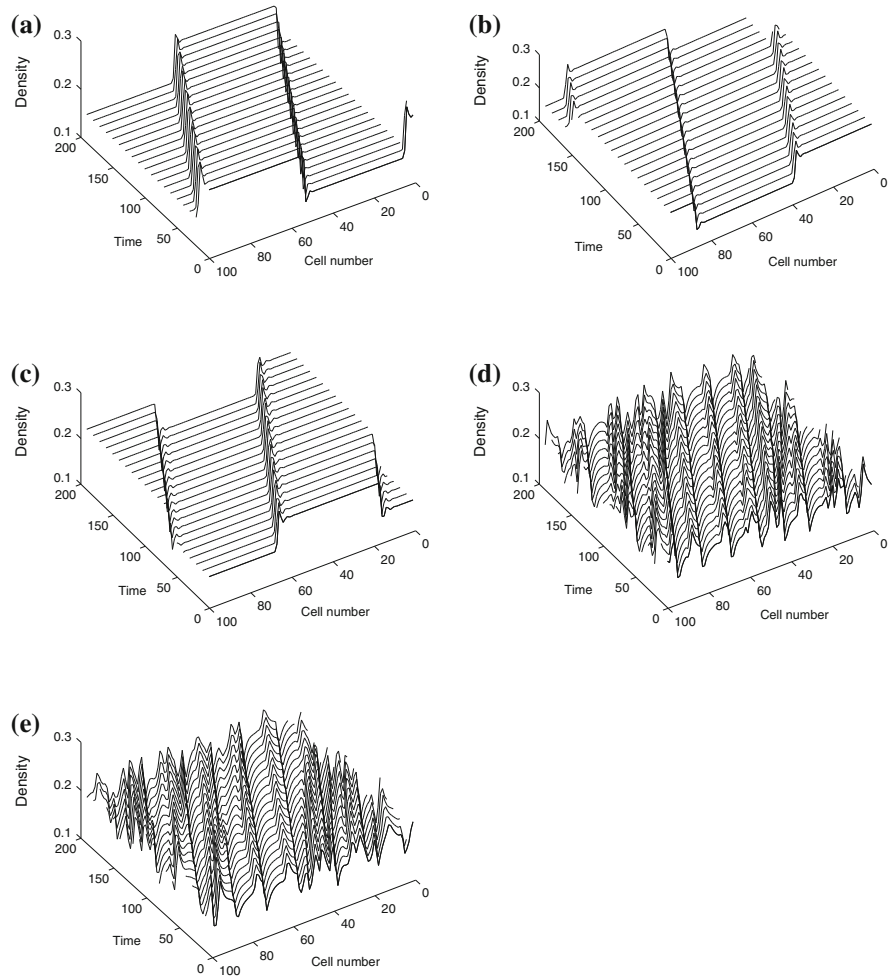
$$\rho_j(0) = \begin{cases} \rho_0 - \sigma; \ 0 \leq j < \frac{L}{2} \\ \rho_0 + \sigma; \ \frac{L}{2} \leq j < L \end{cases}$$

and

$$\rho_j(1) = \begin{cases} \rho_0 - \sigma; \ 0 \leq j < \frac{L}{2} - m, \ L - m \leq jL \\ \rho_0 + \sigma; \ \frac{L}{2} - m \leq j < L - m \end{cases}$$

where σ is the initial disturbance and constant, m is positive integer and L is the total number of sites taken

as 100. The value of the parameters are chosen as:
$\sigma = 0.05$, $m = 0$ and $\rho_0 = \rho_c = 0.2$. From nonlinear
stability analysis, it is derived that kink soliton solu-
tion of mKdV equation exist only for $0 \leq \gamma < \eta(\alpha)$.
Therefore, now presented the discussion on results for
two different range of γ.

Case 1 $\gamma < \eta(\alpha)$

Figure 3 shows the spatiotemporal evolution of den-
sity after sufficiently long time, namely 2×10^4 steps
for different values of α on traffic system when pass-
ing is allowed at a smaller rate. It is clear from the
Fig. 3a–d that initial disturbance leads to the kink soli-
ton which propagates in the backward direction. Due
to this, initial small amplitude disturbance evolves into
congested flow as the instability condition (15) is sat-
isfied. In the stable region, a small amplitude pertur-

bation to the homogeneous density dies out and kink
wave disappears for $\alpha = 0.4$.

Figure 4 describes the density profile at time $t =$
$20,200$ s corresponding to panel of Fig. 3. The region of
free flow turns wide and the amplitude of density waves
is weakened with the increase in anticipation coefficient
which means that anticipation effect enhances the sta-
bility of the traffic flow. For $\alpha = 0.4$, the traffic jam
disappears and flow becomes uniform. Our Numeri-
cal results are consistent with theoretical findings for
$\gamma < \eta(\alpha)$. Therefore, it is reasonable to conclude
that driver's anticipation effect enhances the stability
of traffic flow for smaller rate of passing.

Case 2 $\gamma \geq \eta(\alpha)$

Figure 5 depicts the spatiotemporal evolution of den-
sity for different values of α after sufficiently long

Fig. 6 Density profiles at
time $t = 20,200$ when
$\gamma = 0.3$, $a = 3.1$ for
a $\alpha = 0$, **b** $\alpha = 0.1$,
c $\alpha = 0.2$, **d** $\alpha = 0.3$, and
e $\alpha = 0.4$, respectively
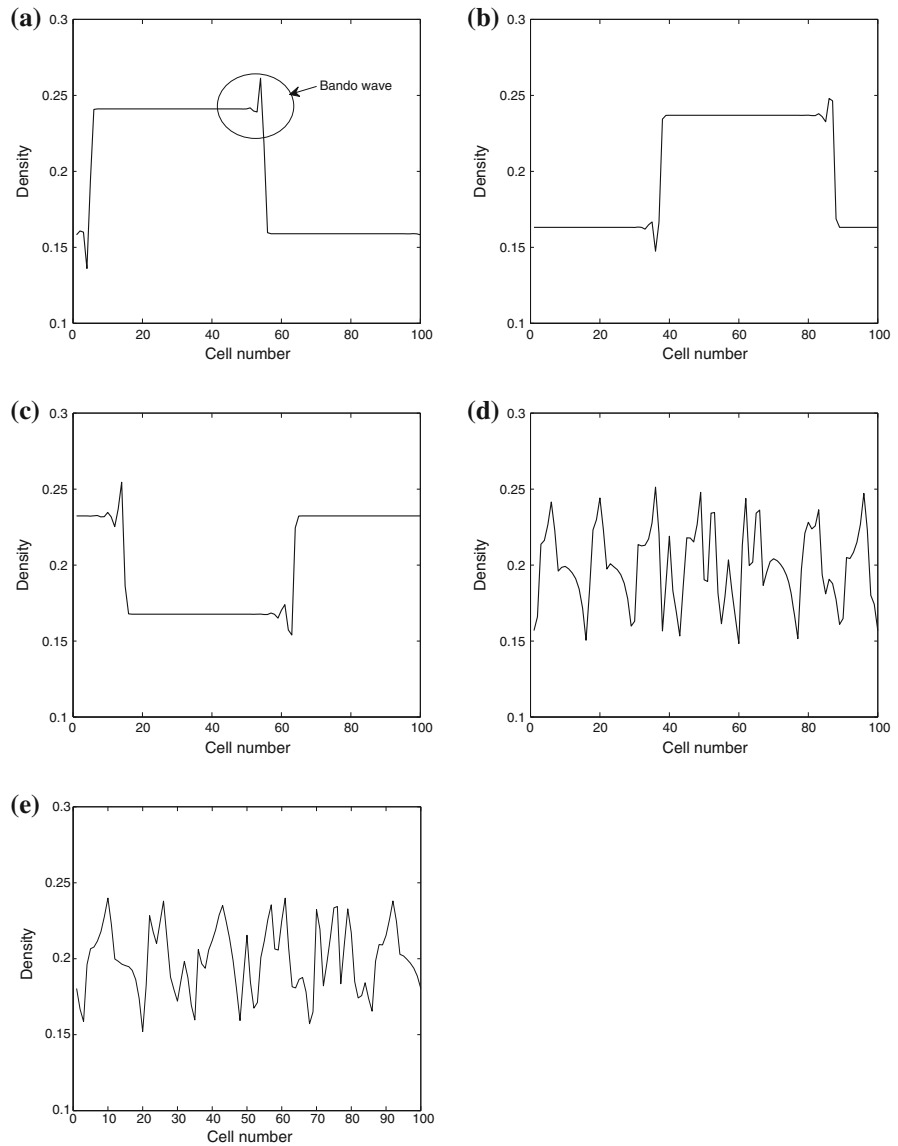
time with passing at higher rate. It is clear from the
figures that the pattern of density profiles is different
for small values of α as compare to those for larger
value of α. From Fig. 5a–c, it is observed that traf-
fic is in kink phase as $a < (3 - 2\alpha)/(1 - 2\eta)$ while
in Fig. 5d, e, the traffic becomes chaotic. Also, in
Fig. 5d, e, the density waves band with one another,
break up and propagates in the backward direction.
From these results, we can conclude that kink as well as
chaotic region exist in the instable region on the phase
plane which also satisfies theoretical results shown in
Fig. 2a.

Figure 6 describes the density profile at time $t =$
20,200 s corresponding to panel of Fig. 5. On com-
paring Fig. 6a–c with Fig. 4a–c, it is observed that the
kink jam profile in larger rate of passing is different
than those obtained for smaller rate of passing. For
$\gamma = 0.3$, the density profile consists of two traveling
waves of different speed, separated by a growing and
decaying region of density. Such nonlinear waves are
knows as a Bando waves [25,26] and highlighted by
circle in the Fig. 6a. On Further increasing the value of
α, these kink-bando wave becomes chaotic wave (see
Fig. 6d, e). These numerical results confirm the theo-

Fig. 7 Plots of density difference $\rho(t) - \rho(t-1)$ vs density $\rho(t)$ when $\gamma = 0.3$, correspond to the panels in Fig. 5, respectively
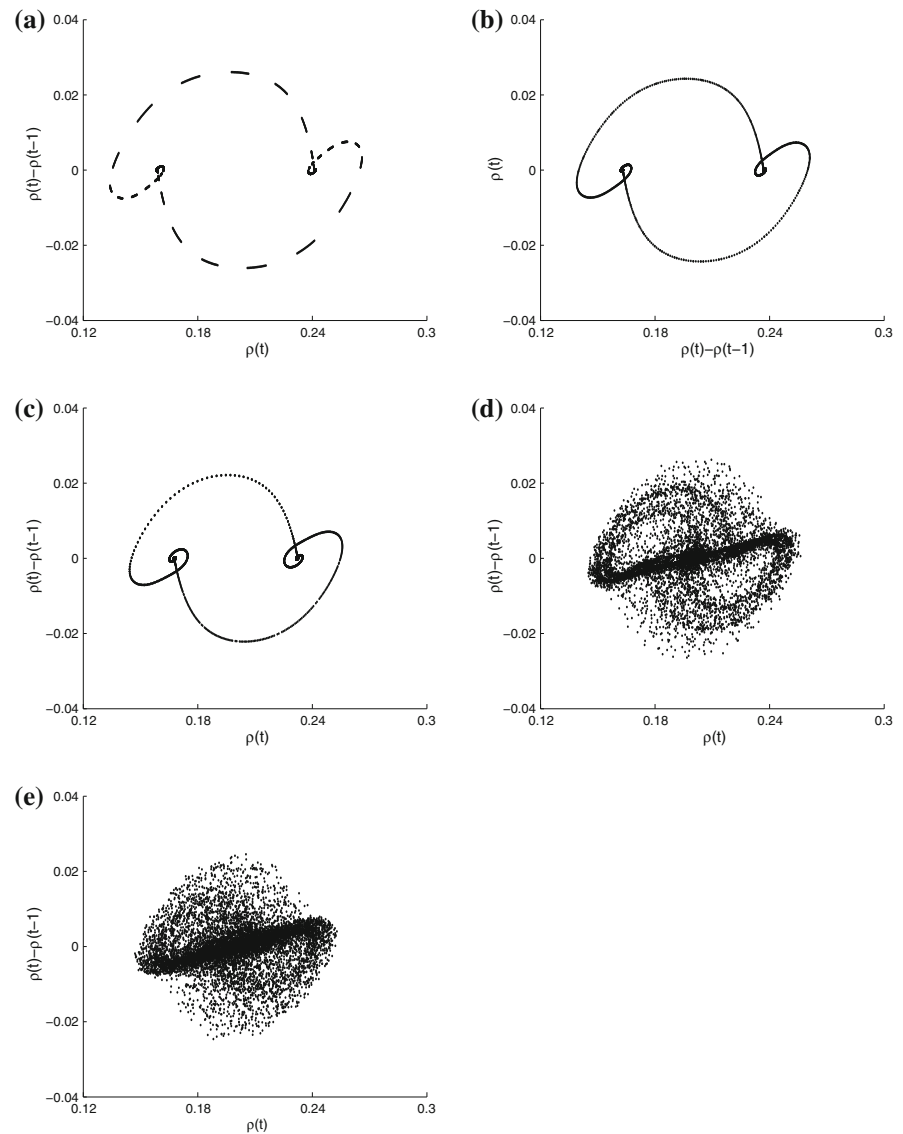
retical findings that for a is less than a_c corresponding to α then traffic is in kink phase while a is greater than a_c, traffic is chaotic and becomes uniform for larger values of a.

To further classify traffic states, we draw phase space plots of density difference $\rho(t) - \rho(t-1)$ against $\rho(t)$ for $t = 20,000 - 30,000$, in Fig. 7 corresponding to the traffic patterns in Fig. 5. The pattern in Fig. 7 represents the set of dispersed points in the phase space plot. For smaller values of α, the pattern exhibits the limit cycle shown in Fig. 7a–c. It corresponds to the periodic traffic

behavior. As α increases, the pattern exhibits dispersed plots around a closed loop which corresponds to the irregular traffic behavior. This chaotic behavior exhibits the behavior characteristics of chaos. The points on the right and left ends represent, respectively, the states within the traffic jams and within the freely moving phase. Therefore, it is reasonable to conclude that the driver's anticipation effect plays a significant role in one dimensional lattice hydrodynamic model with passing and enhances the stability of traffic flow for all possible rates of passing.

6 Conclusion

We proposed a new lattice hydrodynamic model of traffic flow by considering driver's anticipation effect when passing is allowed. The traffic behavior has been analyzed through linear and nonlinear analysis. Through nonlinear stability analysis, we derived the mKdV equation to describe the traffic jam near the critical point and found the condition for which kink soliton solution of mKdV equation exists. For smaller rate of passing, there exist two regions kink jam and no jam on the phase plane while another phase known as chaotic jam exists for larger rate of passing. Phase diagrams are plotted and phase boundary are discussed for smaller and larger rate of passing. It is concluded that anticipation coefficient corresponds to driver's behavior increases significantly the stability of traffic flow for any value of passing constant. The simulation results are compared and found in good accordance with the theoretical findings which verifies that our consideration is reasonable. Therefore, it is worth to conclude that driver's anticipation effect plays an important role in stabilizing the traffic flow and this effect should be considered in traffic flow modeling.

References

1. Jiang, R., Wu, Q.S., Zhu, Z.J.: A new continuum model for traffic flow and numerical tests. Transp. Res. B **36**, 405 (2002)
2. Tang, T.Q., Li, C., Huang, H., Shang, H.: A new fundamental diagram theory with the individual difference of the drivers perception ability. Nonlinear Dyn. **67**, 2255 (2012)
3. Tang, T.Q., Wang, Y.P., Yang, X.B., Wu, Y.H.: A new carfollowing model accounting for varying road condition. Nonlinear Dyn. **70**, 1397 (2012)
4. Tang, T.Q., Shi, Y.F., Wang, Y., Yu, G.: A bus-following model with an on-line bus station. Nonlinear Dyn. **70**, 209 (2012)
5. Tang, T.Q., Li, C., Huang, H., Shang, H.: A new pedestrian-following model for aircraft boarding and numerical tests. Nonlinear Dyn. **67**, 437 (2012)
6. Gupta, A.K., Katiyar, V.K.: Analyses of shock waves and jams in traffic flow. Phys. A **38**, 4069 (2005)
7. Nagatani, T.: TDGL and MKdV equations for jamming transition in the lattice models of traffic. Phys. A **264**, 581 (1999)
8. Nagatani, T.: Jamming transition in a two-dimensional traffic flow model. Phys. Rev. E **59**, 4857 (1999)
9. Gupta, A.K., Redhu, P.: Jamming transition of a two-dimensional traffic dynamics with consideration of optimal current difference. Phys. Lett. A **377**, 2027 (2013)
10. Tang, T.Q., Li, C.Y., Huang, H.J.: A new car-following model with the consideration of the drivers forecast effects. Phys. Lett. A **374**, 3951 (2010)
11. Tang, T.Q., Huang, H.J., Shang, H.Y.: A new macro model for traffic flow with the consideration of the drivers forecast effect. Phys. Lett. A **374**, 1668 (2010)
12. Tian, J.F., Jia, B., Li, X.G., Gao, Z.Y.: Flow difference effect in the lattice hydrodynamic model. Chin. Phys. B **19**, 040303 (2010)
13. Nagatani, T.: Modified KdV equation for jamming transition in the continuum models of traffic. Phys. A **261**, 599 (1998)
14. Ge, H.X., Cheng, R.J.: The backward looking effect in the lattice hydrodynamic model. Phys. A **387**, 6952 (2008)
15. Peng, G.H., Cai, X.H., Cao, B.F., Liu, C.Q.: Non-lane-based lattice hydrodynamic model of traffic flow considering the lateral effects of the lane width. Phys. Lett. A **375**, 2823 (2011)
16. Peng, G.H., Cai, X.H., Liu, C.Q., Tuo, M.X.: A new lattice model of traffic flow with the anticipation effect of potential lane changing. Phys. Lett. A **376**, 447 (2011)
17. Peng, G.H.: A new lattice model of traffic flow with the consideration of individual difference of anticipation driving behavior. Commun. Nonlinear Sci. Numer. Simul. **18**, 2801 (2013)
18. Kang, Y.R., Sun, D.H.: Lattice hydrodynamic traffic flow model with explicit drivers physical delay. Nonlinear Dyn. **71**, 531 (2013)
19. Nagatani, T.: Jamming transitions and the modified Korteweg-de Vries equation in a two-lane traffic flow. Phys. A **265**, 297 (1999)
20. Peng, G.H.: A new lattice model of two-lane traffic flow with the consideration of optimal current difference. Commun. Nonlinear Sci. Numer. Simul. **265**, 297 (2012)
21. Tao, W., Gao, Z.Y., Zhao, X.M., Tian, J.F., Zhang, W.Y.: Flow difference effect in the two-lane lattice hydrodynamic model. Chin. Phys. B **21**, 070507 (2012)
22. Gupta, A.K., Redhu, P.: Analysis of a modified two-lane lattice model by considering the density difference effect. Commun. Nonlinear Sci. Numer. Simul. **19**(5), 1600–1610 (2013)
23. Peng, G.H.: A new lattice model of the traffic flow with the consideration of the driver anticipation effect in a two-lane system. Nonlinear Dyn. **73**, 1035–1043 (2013). doi:10.1007/s11071-013-0850-7
24. Gupta, A.K., Redhu, P.: Analyses of drivers anticipation effect in sensing relative flux in a new lattice model for two-lane traffic system. Phys. A **392**, 5622 (2013)
25. Nagatani, T.: Chaotic jam and phase transition in traffic flow with passing. Phys. Rev. E **60**, 1535 (1999)
26. Tang, C.F., Jiang, R., Wu, Q.S.: Phase diagram of speed gradient model with an on-ramp. Phys. A **377**, 641 (2007)
27. Berg, P., Mason, A., Woods, A.: Continuum approach to car-following models. Phys. Rev. E **61**, 1056 (2000)